npj | vaccines

Article

Published in partnership with the Sealy Institute for Vaccine Sciences

https://doi.org/10.1038/s41541-025-01283-x

To generate functional anti-protease-activated receptor-4 (PAR4), a G protein-coupled receptor, antibodies through PAR4-mRNA-LNP immunization

En-Shuo Liu[1,2,12], Kai-Wen Ho[2,12] ✉, Chin-Chung Wu[3], Hsiao-Li Fan[2], Ting-Yu Wang[3], Yuan-Chin Hsieh[4,5], Bo-Cheng Huang[2,6], Shih-Ting Hong[2], Tzu-Yi Liao[1,2], Yen-Ling Liu[1,2], Yu-Tung Chen[1,2], Chia-Ching Lee[1,2], Chiao-Yun Chen[2,7,8], Chih-Lung Lin[1,9,10] ✉ & Tian-Lu Cheng[1,2,11] ✉

G protein-coupled receptors (GPCRs) are key therapeutic targets for various diseases, such as the thrombin receptor protease-activated receptor 4 (PAR4) involved in thrombotic cardiovascular disorders. However, the structural complexity of native GPCRs hinders recombinant protein production, making peptide-based immunization insufficient for generating high-quality antibodies. Here, we developed a PAR4-mRNA-LNP vaccine to express native PAR4 in vivo, thereby inducing potent and specific anti-PAR4 antibodies. The PAR4-mRNA-LNP formulation showed 93.44% encapsulation efficiency, an average size of 127.5 nm, and a polydispersity index (PDI) of 0.1033. Native 55-kDa PAR4 protein with complete glycosylation was confirmed on the cell surface using western blotting and flow cytometry. Mice immunized with PAR4-mRNA-LNP produced strong anti-PAR4 antibody responses, as detected by cell-based ELISA. Finally, we established hybridoma cell lines and identified five clones that significantly inhibited PAR4-mediated platelet aggregation. These findings suggest that mRNA-LNP technology can be broadly applied to generate functional anti-GPCR antibodies for therapy.

G protein-coupled receptors (GPCRs) play important roles in various physiological processes, including sensory perception[1], neurotransmitter[2], and hormone regulation[3]. Dysregulation or abnormal GPCR signaling is associated with various diseases, such as cancer[4], cardiovascular disorders[5], and neurological conditions[6]. Because of their role in disease progression, GPCRs are important therapeutic targets. For example, protease-activated receptor 4 (PAR4) is a GPCR required for platelet activation and has a significant role in cardiovascular diseases, such as myocardial infarction and stroke. Therefore, targeting PAR4 with therapeutic antibodies represents a promising approach. Developing antibodies against GPCRs is challenging because of their structural complexity, which limits recombinant protein production[7]. Peptides are often used as substitutes, but their poor mimicry of the GPCR structure reduces binding specificity and antibody effectiveness[8–10]. Innovative strategies are essential to preserve the native structure of GPCRs. Huang et al. used murine 3T3 cells expressing human CXCR2 with membrane-bound GM-CSF as an adjuvant to enhance antibody production by stimulating local inflammation and splenocyte proliferation[11]. However, this approach may increase background noise,

[1]Graduate Institute of Medicine, College of Medicine, Kaohsiung Medical University, Kaohsiung, Taiwan. [2]Drug Development and Value Creation Research Center, Kaohsiung Medical University, Kaohsiung, Taiwan. [3]Graduate Institute of Natural Products, Kaohsiung Medical University, Kaohsiung, Taiwan. [4]School of Medicine for International Students, I-Shou University, Kaohsiung, Taiwan. [5]Department of Occupational Therapy, I-Shou University, Kaohsiung, Taiwan. [6]Department of Surgery Faculty of Medicine College of Medicine, Kaohsiung Medical University, Kaohsiung, Taiwan. [7]School of Post-Baccalaureate Medicine, College of Medicine, Kaohsiung Medical University, Kaohsiung, Taiwan. [8]Department of Medical Imaging, Kaohsiung Medical University Hospital, Kaohsiung, Taiwan. [9]Department of Neurosurgery, Kaohsiung Medical University Hospital, Kaohsiung, Taiwan. [10]Department of Surgery, School of Medicine, College of Medicine, Kaohsiung Medical University, Kaohsiung, Taiwan. [11]Department of Biomedical Science and Environmental Biology, Kaohsiung Medical University, Kaohsiung, Taiwan. [12]These authors contributed equally: En-Shuo Liu, Kai-Wen Ho.
✉e-mail: kevin79512003@gmail.com; cllin@kmu.edu.tw; tlcheng5024@gmail.com

resulting in a weakening of the immune response and complicating the identification of specific antibodies. Therefore, a strategy to enhance GPCR antibody generation is needed that can maintain the native GPCR structure, reduce background noise, and act as a good adjuvant to produce a strong antibody response.

During the COVID-19 pandemic, mRNA-LNP technology gained prominence as a platform for delivering lipid nanoparticle–encapsulated mRNA, enabling intracellular expression of target proteins in vivo—often in a membrane-embedded, glycosylated, and conformationally correct state[12–14]. Unlike recombinant protein purification methods, which can disrupt native protein conformations—particularly for complex transmembrane proteins such as GPCRs—mRNA-LNPs promote protein synthesis within a physiological environment, thereby preserving membrane topology, glycosylation, and receptor functionality. In addition, the mRNA itself acts as a potent adjuvant by activating toll-like receptors 7 and 8 (TLR7/8), thereby inducing a strong immune response and promoting the generation of antigen-specific antibodies[15]. Based on this strategy, we developed PAR4-expressing mRNA-LNPs (PAR4-mRNA-LNPs) to immunize BALB/c mice and employed a hybridoma approach[16] to generate functional anti-PAR4 antibodies (Fig. 1). Initially, the structural integrity and synthesis efficiency of PAR4-mRNA-LNP had been confirmed via gel electrophoresis and particle characterization. Subsequently, we verified the molecular weight and surface expression of PAR4 on 293 T cells after PAR4-mRNA-LNP using western blotting and flow cytometry, respectively. Throughout the immunization timeline in BALB/c mice, antibody responses had been quantified by PAR4-expressing cell-based ELISA, monitoring response escalation following sequential boosts. To establish sustained antibody production, hybridoma clones had been generated and screened, confirming anti-PAR4 IgG/IgM and isotypes. Functional inhibition assays evaluated the antagonistic capability of anti-PAR4 antibodies on platelet aggregation. This mRNA-LNP approach enhanced antibody specificity and efficacy by preserving the native GPCR structure and resulted in the production of high-quality, functional antibodies.

Results

Characterization of the PAR4-mRNA-LNP

To express native PAR4 on the cell surface in vivo, we designed a human PAR4 (a type of GPCR) mRNA that contained the PAR4 signal peptide along with the full-length human PAR4 gene to facilitate surface expression and a Flag-tag for detection. In addition, the 5' cap, UTR, and poly (A) tail were synthesized on the mRNA of PAR4 to optimize its stability and transcription efficiency[17,18] (Fig. 2A). To confirm that the PAR4 mRNA was successfully constructed, 1,182 base pairs were detected using agarose gel electrophoresis (Fig. 2B, complete figure on Supplementary Fig. 1). Next, we encapsulated the mRNA of PAR4 into lipid nanoparticles (LNP) to form PAR4-mRNA-LNP. The encapsulation efficiency of PAR4-mRNA-LNP was 93.44%, the mean size was 127.5 nm, and the PDI was 0.1033, which complies with FDA guidelines (PDI should remain below 0.3)[19]. The results indicated that all nanoparticles were of similar size and demonstrated a monodispersed size distribution (Fig. 2C). Thus, the PAR4-mRNA-LNP was successfully developed and ready for cell transfection and PAR4 surface expression.

PAR4 surface expression following PAR4-mRNA-LNP transfection

To confirm PAR4-mRNA-LNP-expressing native PAR4 on the cell surface, different doses (0.5, 1, 2 μg) of PAR4-mRNA-LNP were transfected into 293 T cells, and the native structure and surface expression of PAR4 were evaluated by western blot analysis and flow cytometry. For western blot analysis, we used an anti-Flag antibody (clone: 9A3) to verify the correct molecular weight of Flag-PAR4. Two bands were observed at 55 kDa and 40 kDa in the PAR4-expressing cells (293T-Flag-PAR4 cells, used as a positive control), which corresponded to the presence or absence of native PAR4 glycosylation. PAR4-mRNA-LNP effectively expressed a 55 kDa band representing PAR4 with complete glycosylation in a dose-dependent manner (Fig. 3A, complete figure on supplementary figure 2). To further assess the surface expression of PAR4, the 293T-Flag-PAR4 group and different transfection doses of PAR4-mRNA-LNP were analyzed using a commercial anti-PAR4 antibody (clone: 5F10) and evaluated by flow cytometry. The results indicated that both 293T-Flag-PAR4 cells and different transfection amounts of PAR4-mRNA-LNP increased the intensity of FITC fluorescence, which confirmed surface PAR4 expression in a dose-dependent manner (Fig. 3B). The results indicated that PAR4-mRNA-LNP results in complete glycosylation of native PAR4 on the cell surface.

Anti-human PAR4 antibody responses following PAR4-mRNA-LNP immunization

BALB/c mice ($n = 6$) were administered three intramuscular injections of 10 μg PAR4-mRNA-LNP, followed by a final (4th) 3 μg boost. Serum was collected during the 2nd, 3rd, and final boosts to measure anti-PAR4 antibody responses. PAR4-expressing cells were seeded into a 96-well plate and various dilutions of mouse serum were added to screen for anti-PAR4 antibody responses using horseradish peroxidase (HRP)-conjugated anti-mouse IgG antibody. The results indicated that anti-PAR4 antibodies were produced in two mice (No. mouse-2 and mouse-5) after the 2nd boost (Fig. 4A). Following the 3rd boost, five mice produced anti-PAR4 antibody responses (Fig. 4B). After the final boost (4th), all mice exhibited anti-PAR4 antibody responses. Notably, 5 of 6 mice produced high antibody responses

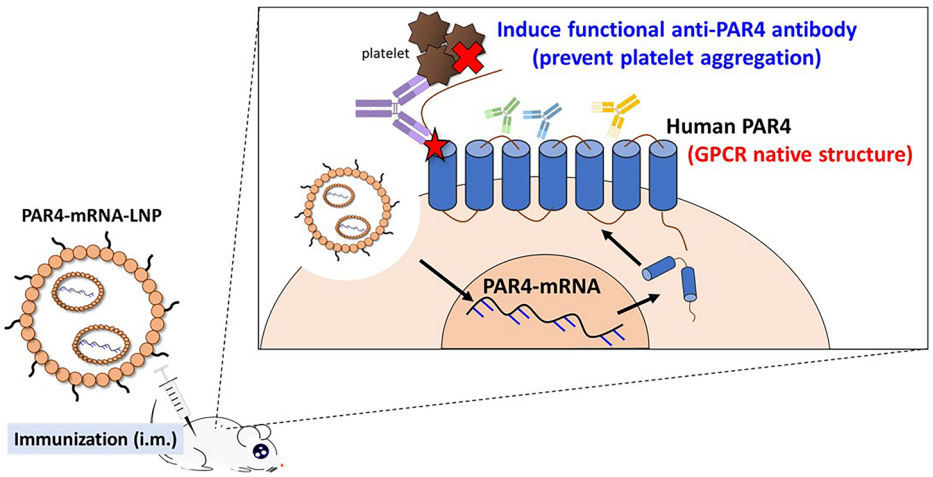

Fig. 1 | PAR4-mRNA-LNP immunization can generate functional anti-PAR4 antibodies to prevent platelet aggregation. We developed human PAR4-mRNA-LNPs to immunize mice via intramuscular injections, enabling the transfection of PAR4-mRNA into mouse cells in vivo. This resulted in the surface expression of the native human PAR4 structure, effectively inducing an antibody response and leading to the generation of various anti-human PAR4 antibodies. We selected the most effective functional anti-PAR4 antibody to serve as a PAR4 antagonist, which was capable of inhibiting platelet aggregation.

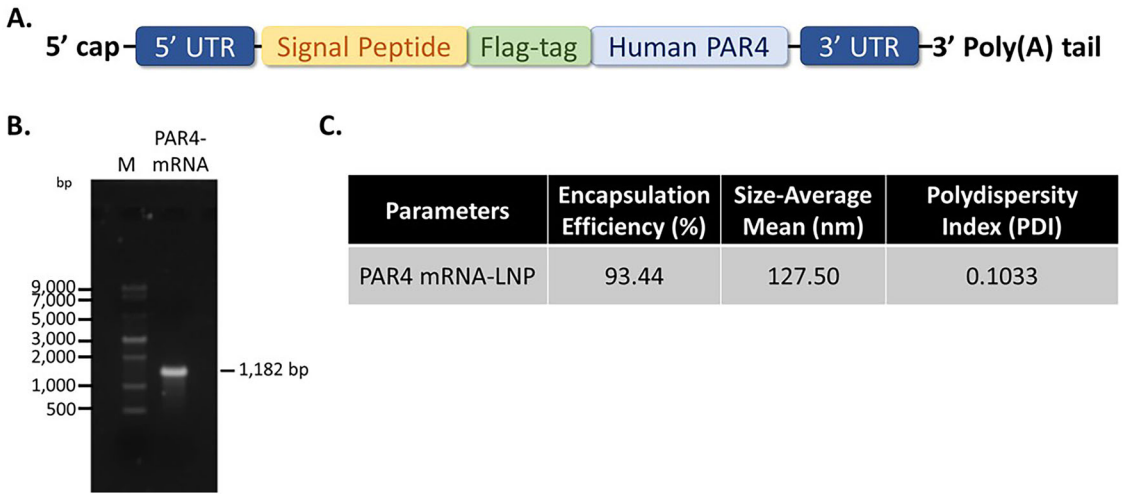

C.

Parameters	Encapsulation Efficiency (%)	Size-Average Mean (nm)	Polydispersity Index (PDI)
PAR4 mRNA-LNP	93.44	127.50	0.1033

Fig. 2 | Characterization of PAR4-mRNA-LNP. A Schematic of the PAR4 mRNA sequence design, which consists of the full-length human PAR4 gene, the PAR4 signal peptide, and a Flag-tag for PAR4 surface expression. The 5′ cap, 5′ UTR, 3' UTR, and poly(A) tail were optimized for stability and transcription efficiency. **B** The mRNA of PAR4 (1,182 base pairs, bp) was detected using agarose gel electrophoresis. M: RNA ladder. **C** The parameters of PAR4-mRNA-LNP included encapsulation efficiency, size average mean, and polydispersity index (PDI).

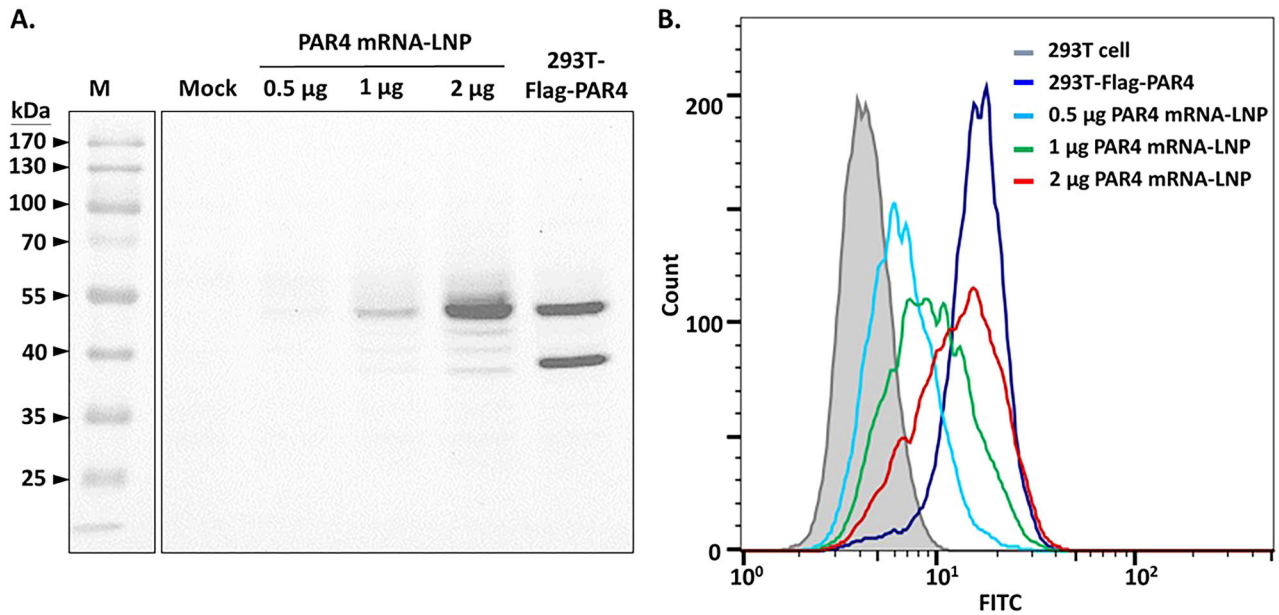

Fig. 3 | PAR4 surface expression following PAR4-mRNA-LNP transfection. We transfected 0.5, 1, and 2 μg of PAR4-mRNA-LNP into 293 T cells. **A** To assess the molecular weight of PAR4, an anti-Flag-tag antibody (clone: 9A3) was used to detect Flag-PAR4. In 293T-Flag-PAR4, which served as a positive control, bands were observed at 40 kDa (representing native PAR4 without glycosylation) and 55 kDa (representing native PAR4 with glycosylation). The PAR4-mRNA-LNP transfection groups exhibited a major band at 55 kDa, indicating the presence of the native PAR4 structure with complete glycosylation. The mock group, which did not receive PAR4-mRNA-LNP, served as a negative control. M: Protein ladder, 10–180 kDa. **B** Surface expression of PAR4 was assessed by flow cytometry using an anti-PAR4 antibody (clone: 5F10, MABS1298). The FITC fluorescence intensity indicated the surface expression of PAR4, which increased in a dose-dependent manner with PAR4-mRNA-LNP transfection. The 293-T cell group acted as a negative control, whereas the 293T-Flag-PAR4 group served as a positive control.

at a 30,000-fold dilution (absorbance 405 nm > 1), with the exception of mouse-3 (absorbance 405 nm < 1) (Fig. 4C). The results indicate that PAR4-mRNA-LNP effectively induces anti-human PAR4 antibodies following immunization.

Establishment of hybridoma cells producing monoclonal anti-PAR4 antibodies

To stably generate monoclonal anti-PAR4 antibodies, we collected splenocytes from mice and fused them with FO myeloma cells at a 4:1 ratio to establish hybridomas using the ECM-2001 Hybridoma System. The fused cells were distributed into 1152 wells in twelve 96-well plates and incubated in HAT medium to select the surviving hybridoma cells and establish single clones. A total of 92 single clones were screened for anti-PAR4 antibodies using a cell-based ELISA and 293T-Flag-PAR4 cells. Fifteen candidate clones were identified. After incubating the clones in a 6-well plate, they were tested with horseradish peroxidase (HRP)-conjugated IgG + IgM antibody to confirm the production of anti-PAR4 antibodies. The results indicated that 13 of the 15 hybridoma clones produced anti-PAR4 IgG or

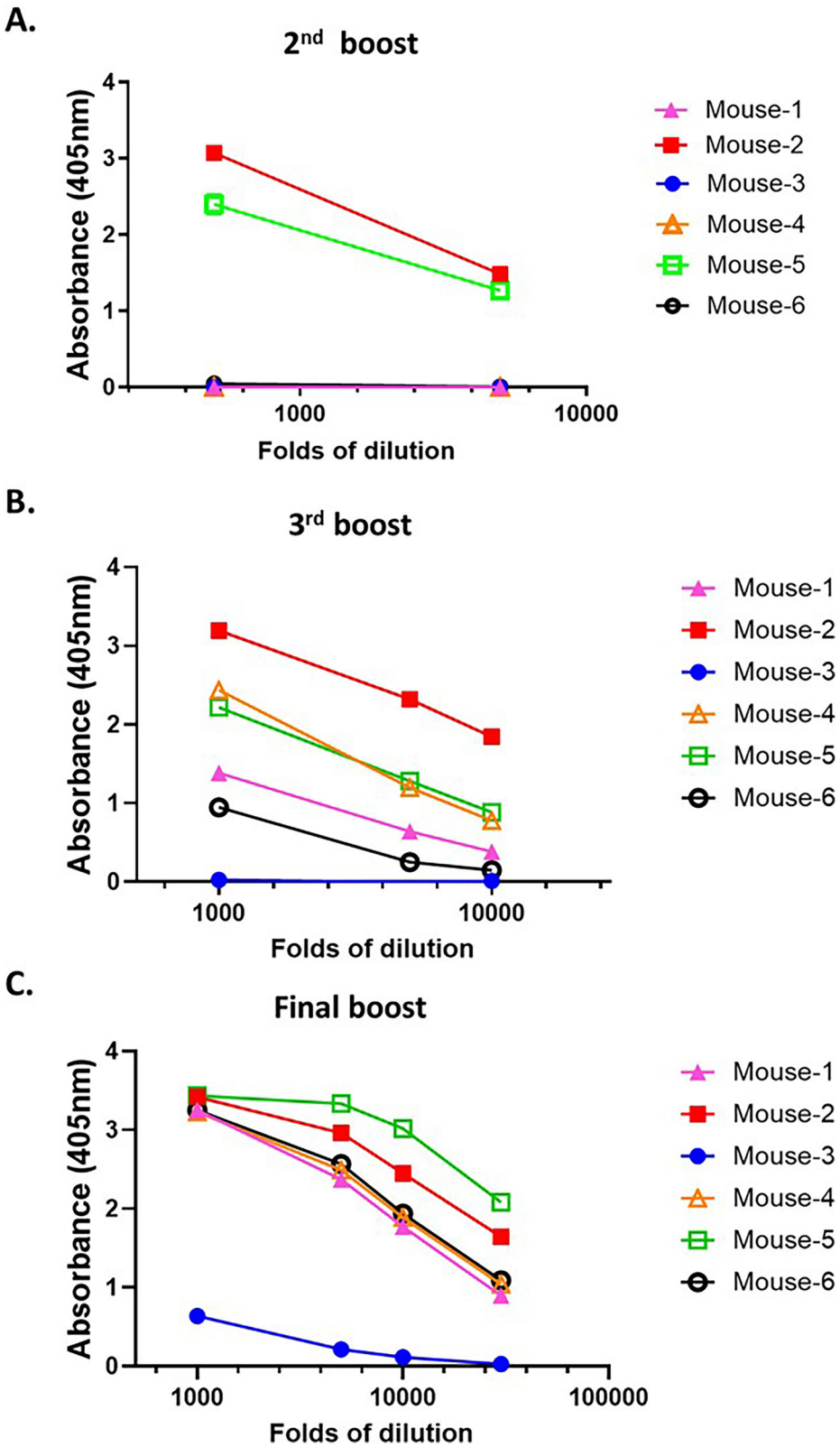

Fig. 4 | Anti-human PAR4 antibody responses following PAR4-mRNA-LNP immunization. After immunizing BALB/c mice ($n = 6$) with PAR4-mRNA-LNP through intramuscular injection, a PAR4-expressing cell-based ELISA was used to measure the anti-PAR4 antibody responses with horseradish peroxidase (HRP)-conjugated anti-mouse IgG antibody for detection. **A** Following the 2nd boost, two mice exhibited anti-PAR4 antibody responses. **B** After the 3rd boost, five mice produced anti-PAR4 antibody responses. **C** Following the final boost, all mice exhibited anti-PAR4 antibody responses; specifically, mice 1, 2, 4, 5, and 6 displayed extremely high PAR4 antibody responses, even at a 30,000-fold dilution.

IgM (Fig. 5A). To identify the isotypes of the anti-PAR4 antibodies, an HRP-conjugated anti-mouse IgG antibody was used to determine the presence of anti-PAR4 mouse IgG. Consequently, 10 of the 15 hybridoma clones generated anti-PAR4 IgG (Fig. 5B). Both assays showed no non-specific binding in 293-T cells, confirming the successful establishment of hybridoma cells that stably express specific anti-PAR4 IgG and IgM.

Screening of the functional anti-PAR4 antagonist antibody and identification of its isotype

To determine whether the 13 anti-PAR4 IgG and IgM antibodies from Fig. 5 act as PAR4 antagonists to inhibit PAR4-mediated platelet aggregation, we pretreated human platelet suspensions with the antibodies, followed by stimulation with 100 μM protease-activated receptor 4 agonist peptide (PAR4-

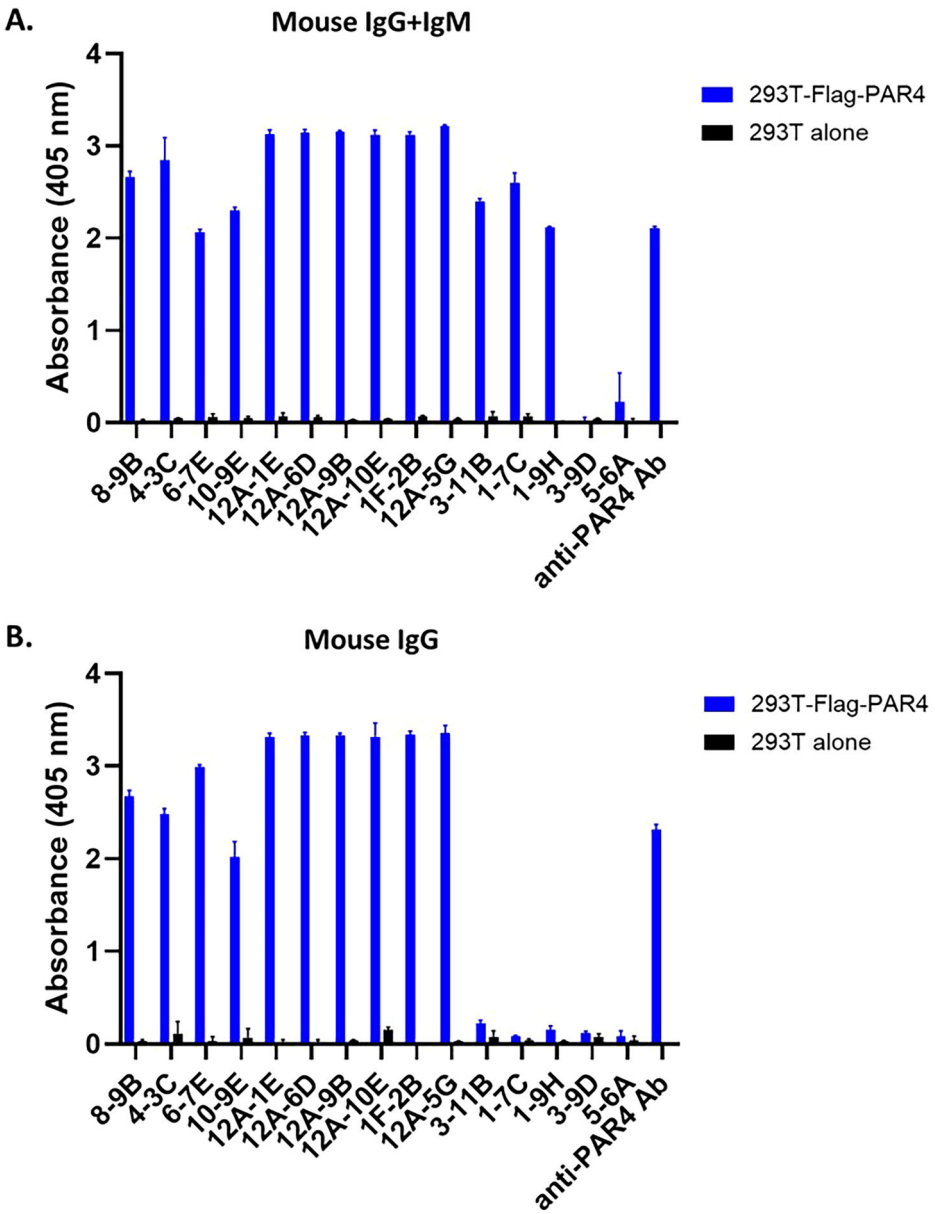

Fig. 5 | PAR4-expressing cell-based ELISA to evaluate anti-PAR4 antibody from hybridoma cells. Fifteen clones were screened using a PAR4-expressing and 293 T alone cell-based ELISA. **A** The anti-PAR4 antibodies were measured using HRP-conjugated anti-mouse IgG + IgM. **B** The HRP-conjugated anti-mouse IgG Fc fragment identified the isotypes of the anti-PAR4 antibodies in the supernatants from each hybridoma cell. Thirteen hybridoma clones produced high levels of specific anti-PAR4 IgG (10 clones) or IgM (3 clones). Anti-PAR4 Ab served as a positive control.

AP). If the anti-PAR4 antibodies act as antagonists, they may compete with PAR4-AP to inhibit platelet aggregation. The results indicated that five functional anti-PAR4 IgG antibodies (8-9B, 1F-2B, 12A-6D, 12A-9B, and 12A-10E) inhibited platelet aggregation in the presence of PAR4-AP. Notably, clones 8-9 B and 12A-10E completely inhibited platelet aggregation and inhibited PAR4-mediated aggregation (Fig. 6A, Supplementary Fig. 3). PAR1-AP was used to confirm the specificity of the five anti-PAR4 IgG antibodies for PAR4 compared with other platelet-agonist receptors. The antibodies had no significant effect on inhibiting PAR1-AP (5 μM)-induced platelet aggregation (Fig. 6B). Moreover, we confirmed that the five anti-PAR4 antibodies specifically bind to native PAR4 on the surface of 293T-PAR4 cells by confocal microscopy (Supplementary Fig. 4). Finally, we determined the mouse IgG isotype of the PAR4 antagonist antibodies (8-9B, 1F-2B, 12A-6D, 12A-9B, and 12A-10E) using a Mouse Monoclonal Antibody Isotyping Test Kit. Clone 8-9B exhibited an IgG2a isotype with a kappa light chain, whereas the other clones (1F-2B, 12A-6D, 12A-9B, and 12A-10E) were of the IgG2b isotype, also with kappa light chains (Table 1, Supplementary Fig. 5). Taken together, these findings suggest that PAR4-mRNA-LNP can immunize mice and induce PAR4 antagonist IgG antibodies.

Discussion

We describe a PAR4-mRNA-LNP approach that efficiently generates high-responses, functional anti-PAR4 antibodies, and overcomes the structural and specificity challenges of GPCRs. The adjuvant properties of mRNA-LNP further enhance the immune response, and mRNA can be used to express any complex protein (like GPCRs). for antibody development through in vivo expression. This simple and convenient mRNA-LNP strategy will accelerate the development of any targeted antibody, particularly against complex proteins.

The mRNA of mRNA-LNP acts as an adjuvant and is potentially recognized by toll-like receptors 7 and 8 (TLR7/8) in the endosomes, which triggers an immune response and affects vaccine effectiveness[20–24]. Upon activation, TLR7/8 recruits the adaptor protein MyD88, which leads to the activation of the transcription factor NF-κB[25–28] and plays an important role in B cell activation by promoting B cell proliferation, differentiation, and antibody production, thereby driving an effective immune response[29–32]. Therefore, mRNA-LNP technology is widely used for vaccines and is effective against COVID-19 and other infectious diseases, such as Zika, HIV, and influenza[33–37] by triggering a strong immune response. Our results show

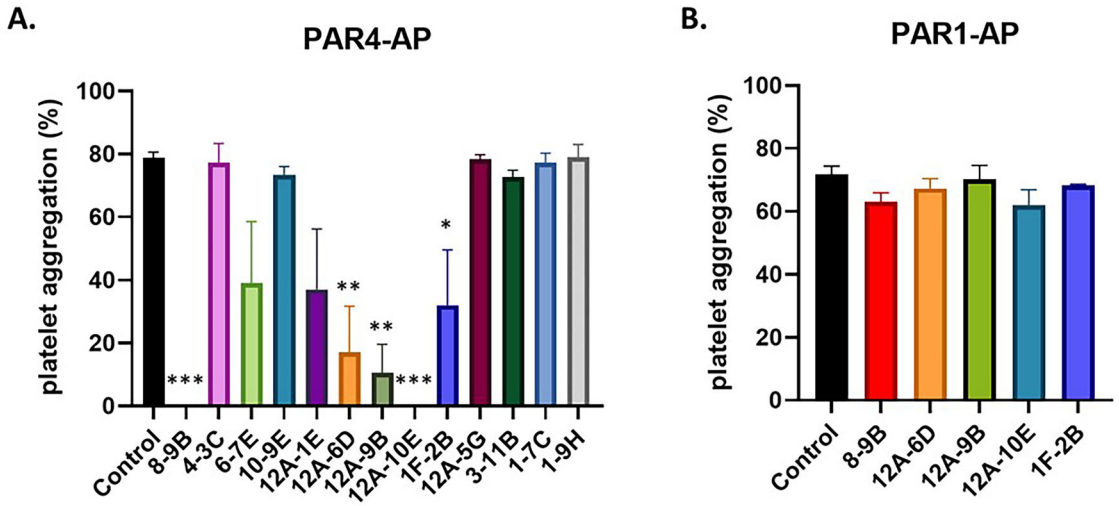

Fig. 6 | Selective inhibition of 13 anti-PAR4 IgG and IgM antibodies on PAR4-mediated human platelet aggregation. To determine whether the functional anti-PAR4 antibodies can inhibit platelet aggregation, **A** human platelet suspensions were pretreated with 13 supernatants from the hybridoma cells for 3 min and stimulated with PAR4-AP (100 μM). Five clones (8-9B, 1F-2B, 12A-6D, 12A-9B, and 12A-10E) were identified as capable of inhibiting platelet aggregation and acting as PAR4 antagonists. **B** To confirm the specificity of the five clones for PAR4 versus other platelet-agonist receptors, PAR1-AP was used. They all showed an inhibitory effect of less than 20% or did not affect PAR1-AP-induced platelet aggregation. Control: FO cell culture medium. Values are presented as the mean ± S.E.M. ($n \geq 3$). $^{*}P < 0.05$, $^{**}P < 0.01$, $^{***}P < 0.001$, compared with the control.

Table 1 | Mouse IgG antibody isotypes of the hybridoma clones

Clone	Mouse IgG isotype	Mouse light chain isotype
8-9B	IgG2a	Kappa
12A-10E	IgG2b	Kappa
12A-9B	IgG2b	Kappa
12A-6D	IgG2b	Kappa
1F-2B	IgG2b	Kappa

The mouse IgG isotype of five anti-PAR4 antagonist antibodies was identified using a Mouse Monoclonal Antibody Isotyping Test Kit. Clone 8-9 B exhibited the IgG2a isotype, whereas the other clones (1F-2B, 12A-6D, 12A-9B, and 12A-10E) were of the IgG2b isotype. All five clones were kappa light chain antibodies.

that following the 4th booster, antibody responses remained significantly strong and maintained effectiveness even when diluted 30,000-fold. This highlights the potential of our approach to generate high antibody responses, which are well-suited for efficient hybridoma screening during subsequent stages. Overall, the PAR4-mRNA-LNP platform streamlines antibody development and leverages the adjuvant properties of mRNA-LNPs to activate TLR7/8, enhancing the immune response, and enabling the production of high-responses, specific antibodies against complex GPCR proteins.

mRNA-LNP technology provides a convenient and versatile alternative to traditional GPCR protein production methods and bypasses the need for detergent solubilization and complex purification steps[38,39]. Traditional approaches face significant challenges, such as turkey β1-adrenergic receptor (β1AR), human adenosine A2A receptor (A2AR), and rat neurotensin receptor (NTSR1), which must be solubilized from the cell surface using detergents, a process that can disrupt the protein's native structure and reduce its functionality[38–41]. Affinity purification is required to isolate the GPCR; however, this step can be complicated by the presence of contaminants or improperly folded proteins[42,43]. Our PAR4-mRNA-LNP strategy addresses traditional challenges by delivering mRNA directly into cells, where PAR4 is naturally synthesized, properly folded, and fully glycosylated on the cell surface. This approach preserves the structural integrity of PAR4, ensures it remains in its native conformation, and significantly streamlines the production of antibodies against complex GPCR targets. In addition, mRNA-LNP technology has promise for generating antibodies against challenging targets, including unstable multi-pass membrane proteins and glycosylated proteins[43,44], as well as low-immunogenic, low-abundance proteins, such as viral antigens[45–47].

Using the native structure of GPCR as an antigen is essential for accurately screening therapeutic anti-GPCR agonists and antagonists. Traditional selection strategies often involve the use of GPCR peptides or GPCR-expressing virus-like particles (VLPs). For example, Tohidkia et al. used biotinylated peptides from the second extracellular loop of the GPCR cholecystokinin-B receptor (CCK-BR) to screen an anti-GPCR scFv phage library and isolate scFvs that recognized the native receptor[48]. Similarly, Huang et al. synthesized a biotinylated N-terminal peptide of GPCR C5aR to screen an anti-GPCR Fab phage library to produce IgG antibodies with strong binding to C5aR-expressing cells[49]. However, GPCR peptides often fail to mimic the complex native structure of the target protein, which results in antibodies that recognize linear rather than functional conformational epitopes, reducing their specificity and therapeutic efficacy[50,51]. VLP displays GPCRs in a membrane-like environment that closely mimics their natural structure. Ho et al. developed a VLP system in HEK293 cells to efficiently screen anti-GPCR antibodies by analyzing 210 GPCR GALR3 variants for yield, stability, and functionality[52]. However, membrane protein impurities, such as misfolded proteins, present significant challenges in VLP systems and complicate the isolation of highly specific antibodies. Furthermore, the process of isolating VLPs is inherently difficult and complex, which further reduces the yield of therapeutically effective antibodies. To address these limitations, our strategy involves using lentiviruses to stably express GPCRs on the cell surface. This method preserves the native structure of GPCRs, ensuring proper folding, post-translational modifications, and membrane embedding. Figure 5 shows the use of a PAR4-expressing, cell-based ELISA to evaluate anti-PAR4 antibody produced by hybridoma cells. This GPCR-expressing, cell-based system enhances the selection of specific and functional anti-GPCR antibodies, making the process more accessible and efficient for research and therapeutic development.

PAR4 has an important role in platelet activation and thrombo inflammation, and it has emerged as a potential target for anti-thrombotic therapy. Unlike PAR1, which mediates rapid but transient platelet activation, PAR4 is associated with a slower, more sustained response that is essential for

stable thrombus formation[53–55]. Although PAR1 inhibitors, such as Vorapaxar, prevent thrombotic events, they carry significant risks, including hemorrhage, particularly intracranial bleeding[56,57]. This necessitates careful patient selection and monitoring and highlights the need for safer therapeutics that target PAR4. In addition to its distinct signaling characteristics, PAR4 expression is significantly upregulated in various diseased tissues[58–60], including those associated with cardiovascular and thrombo-inflammatory disorders[61–63]. This increased expression underscores the role of PAR4 in disease pathology and reinforces its potential as an effective therapeutic target. Our anti-PAR4 antibody specifically inhibits PAR4-mediated platelet activation, offering an effective approach for the safer management of thromboembolic events and cardiovascular conditions.

In conclusion, our mRNA-LNP strategy provides several key advantages for the development of anti-GPCR antibodies. mRNA-LNP serves as a potent adjuvant that stimulates a strong immune response. This approach is also highly convenient as it only requires in vivo injection to efficiently express the target GPCR. This method preserves the native structure of GPCRs on the cell surface, ensuring proper folding and functionality, which is necessary for generating specific antibodies. In addition, the system maintains the native structure of GPCRs, making it ideal for the efficient screening and selection of therapeutic antibodies. Targeting PAR4, which is a promising candidate for diseases like cardiovascular and inflammatory conditions, further emphasizes the relevance of this approach. Taken together, we believe our strategy has the potential to accelerate the development of GPCR-targeted antibodies for various diseases, such as myocardial infarction, stroke, and cancer-associated thrombosis.

Methods

Cells and reagents

We used 293-T and FO cells for this study. We established 293T-Flag-PAR4 cells that stably expressed Flag-PAR4 on the 293-T cell surface by lentivirus transduction. 293 T cells were seeded at 2×10^5 cells/well in a 6-well plate and cotransfected with 2 μg of pLKO-AS3W-Flag-human PAR4-puro (NCBI Reference Sequence: NM_003950.4), 0.2 μg pMD.G, and 1.8 μg pCMV 8.91 using Lipofectamine™ 2000 Transfection Reagent (Thermo Fisher, Inc). After 7 days, the culture medium was collected and filtered through a 0.22-μm syringe filter, mixed with 8 μg/mL polybrene, and added to 1×10^5 293 T cells for viral infection. The cells were selected with 2 μg/mL puromycin. High-expressing Flag-PAR4 293 T cells were detected using mouse anti-human PAR4 antibody (clone 5F10; MABS1298) (1:50 dilution) and FITC-conjugated goat anti-mouse IgG Fcγ (Jackson Immuno-Research Inc. #115-095-008) (1:20 dilution) and sorted using a MoFlo™ XDP Cell Sorter System (Beckman Colter) to generate 293T-Flag-PAR4 cells. The cells were cultured in DMEM (Sigma-Aldrich) containing 10% heat-inactivated bovine calf serum (GE Healthcare Life Science) and 1% penicillin combined with streptomycin (Thermo Fisher Scientific) at 37 °C in a humidified atmosphere containing 5% CO_2.

Mouse

All BALB/c mice used in this study were obtained from the National Laboratory Animal Center (NLAC), Taiwan. All animal procedures were conducted in accordance with the guidelines approved by the Institutional Animal Care and Use Committee (IACUC) of Kaohsiung Medical University, Taiwan. When animals reached humane endpoints—such as a sudden loss of body weight (>20%), moribund condition, or severely reduced mobility—euthanasia was performed using gradual-fill carbon dioxide (CO_2) inhalation, in compliance with the AVMA Guidelines for the Euthanasia of Animals (2020) and NLAC guideline. The CO_2 flow rate was maintained at 20–30% of the chamber volume per minute to minimize distress. For procedures requiring immediate tissue collection, such as spleen extraction for hybridoma generation, animals were first deeply anesthetized with isoflurane (≥3%) until complete loss of reflexes (e.g., toe-pinch), followed by cervical dislocation performed by trained personnel. This approach adhered to institutional IACUC protocols and internationally accepted standards for humane euthanasia.

Design of the PAR4-mRNA-LNP

The PAR4-mRNA-LNP used in this study was synthesized by Dr. Ching-Jen Yang at the Development Center of Biotechnology (DCB), Taiwan, on a contract basis. The PAR4 gene sequence was derived from the NCBI Reference Sequence: NM_003950.4. The PAR4-mRNA was modified with a 5′ cap, untranslated regions (UTRs), and a poly(A) tail containing 50 adenosine residues. The mRNA was then encapsulated into lipid nanoparticles (LNPs) using a formulation similar to that used by Moderna, consisting of SM-102 (ionizable lipid), helper lipid, cholesterol, and PEG-lipid in a molar ratio of 50:10:38.5:1.5[64]. The encapsulation efficiency, particle size, and polydispersity index (PDI) were evaluated by Dr. Yang's team using dynamic light scattering (DLS).

Evaluate the PAR4 surface expression of PAR4-mRNA-LNP by western blot analysis and flow cytometry

293-T cells were seeded at 2×10^5/mL in a 12-well growth plate and incubated overnight. The medium was replaced with 750 μL of fresh medium. After 30 min, we added 250 μL of medium containing 0, 0.5, 1, or 2 μg of PAR4-mRNA-LNP to the cells and incubated for 48 h. PAR4 expression was detected by western blot analysis and flow cytometry. PAR4 expression in 293-T cells transfected with PAR4-mRNA-LNP was assessed by western blot analysis. The primary antibody was DYKDDDDK Flag-Tag (9A3) mouse mAb (Cell Signaling Technology, Inc; #8146) and the secondary antibody was Goat anti-mouse IgG Fcγ fragment specific-HRP (Jackson Immuno-Research Inc. #115-035-008). After developing the blot by chemiluminescence, the bands were quantified using a MultiGel-21 UVP imaging system. The surface expression of PAR4 in 293 T cells by flow cytometry following transfection with PAR4-mRNA-LNP and staining the cells with mouse anti-human PAR4 antibody (clone 5F10; MABS1298), followed by incubation with FITC-conjugated goat anti-mouse IgG Fcγ (Jackson Immuno-Research Inc. #115-095-008). The surface fluorescence intensity of viable cells was measured using a Merck Guava easyCyte System flow cytometer and the data were analyzed using FlowJo v10.8.1.

PAR4 antibody responses after immunization with PAR4-mRNA-LNP

BALB/c mice ($n = 6$), aged 6–8 weeks, were immunized with three intramuscular (i.m) injections of 10 μg PAR4-mRNA-LNP, administered once every 2 weeks for 6 weeks. At 8 weeks, a final (4^{th}) intramuscular boost of 3 μg PAR4-mRNA-LNP was administered. Tail vein blood was collected and the serum was stored at −80 °C one week after each booster. Anti-human PAR4 antibody responses from mouse serum were screened using a cell-based ELISA. 293T-Flag-PAR4 cells (1×10^5 cells/well) were seeded in 96-well plates (Thermo Fisher Scientific Inc. #167008) coated with 50 μg/mL poly-D-lysine and incubated overnight. The cells were fixed in 1% paraformaldehyde in PBS for 5 min at room temperature, followed by the addition of 0.1 M glycine to neutralize the paraformaldehyde for 30 min at room temperature. The plates were blocked with 5% milk and diluted anti-human PAR4 antibody from mouse serum (in 2% skim milk) was added to each well and incubated for 50 min at room temperature. Horseradish peroxidase (HRP)-conjugated goat anti-mouse IgG Fcγ fragment specific-HRP (Jackson Immuno-Research Inc. #115-035-008) (1:2000) was added and incubated for 50 min at room temperature. Following three washes with PBS, ABTS, and H_2O_2 were added. The binding capacities of each serum sample were evaluated using an ELISA reader and the data were analyzed using GraphPad Prism software (v10.0).

Establishing a hybridoma using the ECM-2001 Hybridoma System for electrofusion

Splenocytes (1.6×10^7/ml) and FO myeloma cells (4×10^6/ml) were mixed at a 4:1 ratio and washed twice with 20 ml electrofusion medium (centrifuged at 1400 rpm for 7 min). The pellets were resuspended with 2 mL of room temperature Cytofusion Medium C and the pellet was transferred to a 2 mL coaxial chamber. We immediately performed electrofusion (within 30 seconds) using the recommended parameters (Step-1. Pre-AC:

V0 = 40 V, VF = 40 V, T = 15 s, F = 1.4 MHz; Step-2. Pre-AC: V0 = 70 V, VF = 70 V, T = 20 sec, F = 1.4 MHz; DC-PULSE: V = 800 V, T = 40 μs, N = 1, I = 0; Post-AC: V0 = 70 V, VF = 5 V, T = 30 sec, F = 1.4 MHz). Finally, the fusion mixture was plated into twelve 96-well plates (1,152 total wells) and cultured in HAT medium (Sigma-Aldrich) to screen for hybridomas.

Evaluation of anti-PAR4 antibody secreted from hybridoma cells

After establishing hybridoma cells and observing their growth to approximately 50% confluency in 96-well plates over 1–2 weeks, the supernatants were collected and the PAR4 antibodies were determined using a cell-based ELISA. 293T-Flag-PAR4 cells (1×10^5 cells/well) were seeded into 96-well plates (Thermo Fisher Scientific Inc. #167008) coated with 50 μg/mL poly-D-lysine and incubated overnight. The cells were fixed in 1% paraformaldehyde in PBS for 5 min at room temperature, followed by the addition of 0.1 M glycine to neutralize the paraformaldehyde for 30 min at room temperature. The plates were blocked in 5% milk and the supernatants were added to each well for 50 min at room temperature. After three washes with PBS, horseradish peroxidase (HRP)-conjugated goat anti-mouse IgG + IgM (H + L) antibody (Jackson Immuno-Research Inc. #115-035-044) (1:1,000) and horseradish peroxidase (HRP)-conjugated goat anti-mouse IgG Fc fragment antibody (Jackson Immuno-Research Inc. #115-035-008) (1:1,000) were added and incubated for 50 min at room temperature. After three washes with PBS, ABTS and H_2O_2 were added. The binding capacities of each serum were evaluated using an ELISA reader, and the data were analyzed using GraphPad Prism software (v10.0).

Screening for functional anti-PAR4 antagonist antibodies

The protocol for this study was approved by the Institutional Review Board of Kaohsiung Medical University Hospital. Human blood anticoagulated with acid citrate dextrose was obtained from healthy human volunteers, who had not taken any drugs during the previous two weeks. The blood was centrifuged at 450 × *g* for 15 min and the supernatant was obtained as platelet-rich plasma. The platelet-rich plasma was further centrifuged at 1800 × *g* for 15 min in the presence of prostaglandin E1 (0.5 μM). The platelet pellet was washed with Tyrode's solution containing 2 mM Ca^{2+}, 11.1 mM glucose, and 3.5 mg/ml bovine serum albumin and centrifuged at 1200 × *g* for 7 min in the presence of prostaglandin E1 (0.5 μM) and apyrase (0.15 U/ml). The platelet pellet was washed again as described above except for the omission of prostaglandin E1. The washed platelets were suspended in Tyrode's solution at 3×10^8 platelets/mL unless otherwise specified. Platelet aggregation was measured turbidimetrically with a light-transmission aggregometer (Chrono-Log Co., Havertown, PA, USA). The platelet suspension was pretreated with anti-PAR4 antibodies in the supernatant at 37 °C for 3 min while stirring (1200 rpm), and 100 μM of PAR4-agonist peptide (PAR4-AP, sequence: AYPGKF-NH_2) or 5 μM PAR1-agonist peptide (PAR1-AP, sequence: SFLLRN-NH_2) was added to induce platelet aggregation. The extent of platelet aggregation was measured as the maximal increase in light transmission within 5 min following the addition of inducers.

Evaluation of five functional PAR4 antibodies target native PAR4 expressed on the cell surface

293T-Flag-PAR4 cells were seeded onto 18 mm glass coverslips (Matsunami Micro Cover Glass, 18 mm) pre-coated with 20 μg/mL poly-D-lysine and cultured overnight at 37 °C. The following day, cells were fixed with 1% paraformaldehyde (PFA) for 5 minutes at room temperature and neutralized by 0.1 M glycine, then incubated with 500 μL of hybridoma culture supernatants containing one of the five anti-PAR4 monoclonal antibodies for 50 min. After PBS washing, cells were incubated with FITC-conjugated goat anti-mouse IgG Fcγ secondary antibody (Jackson ImmunoResearch. #115-095-008) for 50 min at room temperature in the dark. Nuclei were counterstained with DAPI Fluoromount-G® (SouthernBiotech. #0100-20), and coverslips were mounted onto glass slides. Confocal fluorescence images were acquired using a confocal microscope (LSM 700 Confocal Microscope).

Identification of the mouse IgG isotype of the PAR4 antagonist antibodies

The mouse IgG isotype of the PAR4 antagonist antibodies was determined using the Mouse Monoclonal Antibody Isotyping Test Kit (Bio-Rad). Freshly collected supernatant (150 μL) was pipetted into each development tube and incubated at room temperature for 30 s. The tube was briefly vortexed to ensure that the colored microparticle solution was completely resuspended. An isotypic strip, with a solid red end at the bottom, was placed into each development tube. The results were interpreted after 5–10 min once the positive flow control bands had appeared.

Statistical analyses

Statistical analyses were performed using GraphPad Prism software (v10.0) and FlowJo v10.8.1. The results are expressed as the means ± standard error of the mean (S.E.M.). Data were analyzed by a one-way analysis of variance (ANOVA), followed by Dunnett's multiple comparison post-hoc test. $p < 0.05$ was considered statistically significant.

Data availability

Data is provided within the manuscript or supplementary information files.

Code availability

No code was used in this study.

Received: 28 May 2025; Accepted: 25 September 2025;
Published online: 20 November 2025

References

1. Ahmad, R. & Dalziel, J. E. G protein-coupled receptors in taste physiology and pharmacology. *Front. Pharm.* **11**, 587664 (2020).
2. Kumar, A. & Pluckthun, A. In vivo assembly and large-scale purification of a GPCR - Galpha fusion with Gbetagamma, and characterization of the active complex. *PLoS One* **14**, e0210131 (2019).
3. Feng, Z., Sun, R., Cong, Y. & Liu, Z. Critical roles of G protein-coupled receptors in regulating intestinal homeostasis and inflammatory bowel disease. *Mucosal. Immunol.* **15**, 819–828 (2022).
4. Dorsam, R. T. & Gutkind, J. S. G-protein-coupled receptors and cancer. *Nat. Rev. Cancer* **7**, 79–94 (2007).
5. Wang, J., Gareri, C. & Rockman, H. A. G-protein-coupled receptors in heart disease. *Circ. Res.* **123**, 716–735 (2018).
6. Guerram, M., Zhang, L. Y. & Jiang, Z. Z. G-protein coupled receptors as therapeutic targets for neurodegenerative and cerebrovascular diseases. *Neurochem. Int.* **101**, 1–14 (2016).
7. Hutchings, C. J., Koglin, M. & Marshall, F. H. Therapeutic antibodies directed at G protein-coupled receptors. *MAbs* **2**, 594–606 (2010).
8. Scott, M. J. et al. Rapid identification of highly potent human anti-GPCR antagonist monoclonal antibodies. *MAbs* **12**, 1755069 (2020).
9. Mancia, F. et al. Production and characterization of monoclonal antibodies sensitive to conformation in the 5HT2c serotonin receptor. *Proc. Natl. Acad. Sci. USA* **104**, 4303–4308 (2007).
10. Jiang, Y. et al. Interplay between G protein-coupled receptors and nanotechnology. *Acta Biomater.* **169**, 1–18 (2023).
11. Huang, C. C. et al. Use of syngeneic cells expressing membrane-bound GM-CSF as an adjuvant to induce antibodies against native multi-pass transmembrane protein. *Sci. Rep.* **9**, 9931 (2019).
12. Sharma, P., Hoorn, D., Aitha, A., Breier, D. & Peer, D. The immunostimulatory nature of mRNA lipid nanoparticles. *Adv. Drug Deliv. Rev.* **205**, 115175 (2024).
13. Kon, E., Ad-El, N., Hazan-Halevy, I., Stotsky-Oterin, L. & Peer, D. Targeting cancer with mRNA-lipid nanoparticles: key considerations and future prospects. *Nat. Rev. Clin. Oncol.* **20**, 739–754 (2023).
14. Pilkington, E. H. et al. From influenza to COVID-19: Lipid nanoparticle mRNA vaccines at the frontiers of infectious diseases. *Acta Biomater.* **131**, 16–40 (2021).

15. Li, M. et al. Engineering intranasal mRNA vaccines to enhance lymph node trafficking and immune responses. *Acta Biomater.* **64**, 237–248 (2017).
16. Trier, N. H. & Friis, T. Production of antibodies to peptide targets using Hybridoma Technology. *Methods Mol. Biol.* **2821**, 135–156 (2024).
17. Kim, S. C. et al. Modifications of mRNA vaccine structural elements for improving mRNA stability and translation efficiency. *Mol. Cell Toxicol.* **18**, 1–8 (2022).
18. Gao, M., Zhang, Q., Feng, X. H. & Liu, J. Synthetic modified messenger RNA for therapeutic applications. *Acta Biomater.* **131**, 1–15 (2021).
19. Danaei, M. et al. Impact of particle size and Polydispersity Index on the clinical applications of lipidic nanocarrier systems. *Pharmaceutics* **10**, https://doi.org/10.3390/pharmaceutics10020057 (2018).
20. Coffman, R. L., Sher, A. & Seder, R. A. Vaccine adjuvants: putting innate immunity to work. *Immunity* **33**, 492–503 (2010).
21. Alameh, M. G. et al. Lipid nanoparticles enhance the efficacy of mRNA and protein subunit vaccines by inducing robust T follicular helper cell and humoral responses. *Immunity* **55**, 1136–1138 (2022).
22. Swaminathan, G. et al. A novel lipid nanoparticle adjuvant significantly enhances B cell and T cell responses to sub-unit vaccine antigens. *Vaccine* **34**, 110–119 (2016).
23. Ye, T. et al. CO-DELIVERY of glutamic acid-extended peptide antigen and imidazoquinoline TLR7/8 agonist via ionizable lipid nanoparticles induces protective anti-tumor immunity. *Biomaterials* **311**, 122693 (2024).
24. Ong, E. Z. et al. Immune gene expression analysis indicates the potential of a self-amplifying COVID-19 mRNA vaccine. *NPJ Vaccines* **7**, 154 (2022).
25. Huang, X., Zhang, X. & Lu, M. Recent trends in the development of Toll-like receptor 7/8-targeting therapeutics. *Expert Opin. Drug Discov.* **16**, 869–880 (2021).
26. Braunstein, M. J., Kucharczyk, J. & Adams, S. Targeting toll-like receptors for cancer therapy. *Target Oncol.* **13**, 583–598 (2018).
27. Picard, C., Casanova, J. L. & Puel, A. Infectious diseases in patients with IRAK-4, MyD88, NEMO, or IkappaBalpha deficiency. *Clin. Microbiol Rev.* **24**, 490–497 (2011).
28. Zelkoski, A. E. et al. Ionizable lipid nanoparticles of mRNA vaccines elicit NF-kappaB and IRF responses through toll-like receptor 4. *NPJ Vaccines* **10**, 73 (2025).
29. Gorden, K. B. et al. Synthetic TLR agonists reveal functional differences between human TLR7 and TLR8. *J. Immunol.* **174**, 1259–1268 (2005).
30. Wang, Y. et al. Development of a novel TLR8 agonist for cancer immunotherapy. *Mol. Biomed.* **1**, 6 (2020).
31. Zou, X., Guo, B., Ling, Q. & Mo, Z. Toll-like receptors serve as biomarkers for early diagnosis and prognosis assessment of kidney renal clear cell carcinoma by influencing the immune microenvironment: comprehensive bioinformatics analysis combined with experimental validation. *Front Mol. Biosci.* **9**, 832238 (2022).
32. Yu, H., Lin, L., Zhang, Z., Zhang, H. & Hu, H. Targeting NF-kappaB pathway for the therapy of diseases: mechanism and clinical study. *Signal Transduct. Target Ther.* **5**, 209 (2020).
33. Zhang, C., Maruggi, G., Shan, H. & Li, J. Advances in mRNA Vaccines for Infectious Diseases. *Front Immunol.* **10**, 594 (2019).
34. Richner, J. M. et al. Modified mRNA vaccines protect against Zika Virus Infection. *Cell* **169**, 176 (2017).
35. John, S. et al. Multi-antigenic human cytomegalovirus mRNA vaccines that elicit potent humoral and cell-mediated immunity. *Vaccine* **36**, 1689–1699 (2018).
36. Armbruster, N., Jasny, E. & Petsch, B. Advances in RNA Vaccines For Preventive Indications: A Case Study Of A Vaccine Against Rabies. *Vaccines* **7**, https://doi.org/10.3390/vaccines7040132 (2019).
37. Kiaie, S. H. et al. Recent advances in mRNA-LNP therapeutics: immunological and pharmacological aspects. *J. Nanobiotechnol.* **20**, 276 (2022).
38. Li, X. et al. Heterologous expression and purification of GPCRs. *Methods Mol. Biol.* **2507**, 295–312 (2022).
39. Rasmussen, S. G. et al. Crystal structure of the human beta2 adrenergic G-protein-coupled receptor. *Nature* **450**, 383–387 (2007).
40. Magnani, F. et al. A mutagenesis and screening strategy to generate optimally thermostabilized membrane proteins for structural studies. *Nat. Protoc.* **11**, 1554–1571 (2016).
41. Chun, E. et al. Fusion partner toolchest for the stabilization and crystallization of G protein-coupled receptors. *Structure* **20**, 967–976 (2012).
42. Grisshammer, R. Purification of recombinant G-protein-coupled receptors. *Methods Enzymol.* **463**, 631–645 (2009).
43. Chung, K. Y. et al. Conformational changes in the G protein Gs induced by the beta2 adrenergic receptor. *Nature* **477**, 611–615 (2011).
44. Dodd, R. B., Wilkinson, T. & Schofield, D. J. Therapeutic monoclonal antibodies to complex membrane protein targets: antigen generation and antibody discovery strategies. *BioDrugs* **32**, 339–355 (2018).
45. Zhang, H., Cheng, X., Richter, M. & Greene, M. I. A sensitive and high-throughput assay to detect low-abundance proteins in serum. *Nat. Med* **12**, 473–477 (2006).
46. Pal, S. et al. Intrahepatic hepatitis C virus replication correlates with chronic hepatitis C disease severity in vivo. *J. Virol.* **80**, 2280–2290 (2006).
47. Zhou, H. et al. Generation of monoclonal antibodies against highly conserved antigens. *PLoS One* **4**, e6087 (2009).
48. Tohidkia, M. R., Asadi, F., Barar, J. & Omidi, Y. Selection of potential therapeutic human single-chain Fv antibodies against cholecystokinin-B/gastrin receptor by phage display technology. *BioDrugs* **27**, 55–67 (2013).
49. Huang, L. et al. Discovery of human antibodies against the C5aR target using phage display technology. *J. Mol. Recognit.* **18**, 327–333 (2005).
50. Jo, M. & Jung, S. T. Engineering therapeutic antibodies targeting G-protein-coupled receptors. *Exp. Mol. Med* **48**, e207 (2016).
51. Webb, D. R., Handel, T. M., Kretz-Rommel, A. & Stevens, R. C. Opportunities for functional selectivity in GPCR antibodies. *Biochem Pharm.* **85**, 147–152 (2013).
52. Ho, T. T. et al. Method for rapid optimization of recombinant GPCR protein expression and stability using virus-like particles. *Protein Expr. Purif.* **133**, 41–49 (2017).
53. Rigg, R. A. et al. Protease-activated receptor 4 activity promotes platelet granule release and platelet-leukocyte interactions. *Platelets* **30**, 126–135 (2019).
54. Fender, A. C., Rauch, B. H., Geisler, T. & Schror, K. Protease-activated Receptor PAR-4: an inducible switch between thrombosis and vascular inflammation?. *Thromb. Haemost.* **117**, 2013–2025 (2017).
55. Gnanenthiran, S. R. et al. Identification of a Distinct Platelet Phenotype in the Elderly: ADP Hypersensitivity Coexists With Platelet PAR (Protease-Activated Receptor)-1 and PAR-4-Mediated Thrombin Resistance. *Arterioscler. Thromb. Vasc. Biol.* **42**, 960–972 (2022).
56. Chackalamannil, S. et al. Discovery of a novel, orally active himbacine-based thrombin receptor antagonist (SCH 530348) with potent antiplatelet activity. *J. Med. Chem.* **51**, 3061–3064 (2008).
57. Heuberger, D. M. & Schuepbach, R. A. Protease-activated receptors (PARs): mechanisms of action and potential therapeutic modulators in PAR-driven inflammatory diseases. *Thromb. J.* **17**, 4 (2019).
58. Mitrugno, A. et al. The role of coagulation and platelets in colon cancer-associated thrombosis. *Am. J. Physiol. Cell Physiol.* **316**, C264–C273 (2019).
59. Pavic, G. et al. Thrombin receptor protease-activated receptor 4 is a key regulator of exaggerated intimal thickening in diabetes mellitus. *Circulation* **130**, 1700–1711 (2014).
60. Yu, G. et al. Increased expression of protease-activated receptor 4 and Trefoil factor 2 in human colorectal cancer. *PLoS One* **10**, e0122678 (2015).

61. Mao, Y., Zhang, M., Tuma, R. F. & Kunapuli, S. P. Deficiency of PAR4 attenuates cerebral ischemia/reperfusion injury in mice. *J. Cereb. Blood Flow. Metab.* **30**, 1044–1052 (2010).
62. Edelstein, L. C. et al. Common variants in the human platelet PAR4 thrombin receptor alter platelet function and differ by race. *Blood* **124**, 3450–3458 (2014).
63. Lee, R. H. et al. Investigating the roles of platelet PAR4 in Hemostasis, Thrombosis and viral infection using a newly generated PAR4 floxed mouse. *Blood* **138**, https://doi.org/10.1182/blood-2021-151121 (2021).
64. Zhang, L. et al. Effect of mRNA-LNP components of two globally-marketed COVID-19 vaccines on efficacy and stability. *NPJ Vaccines* **8**, 156 (2023).

Acknowledgements

This work was supported by grants from the Ministry of Science and Technology, Taipei, Taiwan (MOST 111-2314-B-037-051-MY3); the National Science and Technology Council, Taipei, Taiwan (NSTC 112-2320-B-037-011-MY3 and NSTC 112-2124-M-037-001); and the KMU-KMUH Co-Project of Key Research (KMU-DK(B)112001-3) from Kaohsiung Medical University, Taiwan. We also thank the Drug Development and Value Creation Research Center and the Center for Laboratory Animals, Kaohsiung Medical University, Taiwan for the instrumentation and equipment support.

Author contributions

E.S.L. and K.W.H designed and performed experiments reported in the paper analyzed data, and wrote the manuscript; C.C.W. and H.L.F. helped with the platelet aggregation experiments data analysis; T.Y.W. and Y.C.H. helped with the other experiments and data analysis; B.C.H. and S.T.H. contributed to the manuscript editing; T.Y.L. helped with designing human PAR4 plasmid construct; Y.L.L. provided the information of mRNA-LNP immunization; Y.T.C. and C.C.L. provided the information of establishing hybridoma cells; C.Y.C. provided the concept and contributed to manuscript writing and editing; T.L.C. and C.L.L. provided the concept, experimental design and contributed to manuscript writing and editing. All authors read and approved the final manuscript.

Competing interests

The authors declare no competing interests.

Additional information

Supplementary information The online version contains supplementary material available at https://doi.org/10.1038/s41541-025-01283-x.

Correspondence and requests for materials should be addressed to Kai-Wen Ho, Chih-Lung Lin or Tian-Lu Cheng.